



Synthesis and processing effects on magnetic properties in the Fe₅SiB₂ system



B.T. Lejeune^{a, c, *}, R. Barua^{a, c}, I.J. McDonald^{b, c}, A.M. Gabay^d, L.H. Lewis^{a, b, c}, G.C. Hadjipanayis^d

^a Department of Chemical Engineering, Northeastern University, Boston, MA 02115, USA

^b Department of Mechanical & Industrial Engineering, Northeastern University, Boston, MA 02115, USA

^c George J. Kostas Research Institute for Homeland Security, Northeastern University, Burlington, MA 01803, USA

^d Department of Physics, University of Delaware, Newark, DE 19716, USA

ARTICLE INFO

Article history:

Received 15 May 2017

Received in revised form

19 September 2017

Accepted 9 October 2017

Available online 10 October 2017

Keywords:

Fe₅SiB₂

Magnetocrystalline anisotropy

Permanent magnets

Rare-earth-free

ABSTRACT

The effects of Ge substitution and synthesis via rapid solidification on the structure and magnetic character of the intermetallic Fe₅SiB₂ (5-1-2) system were determined, with the objective to investigate the potential of Fe₅(Si_{0.75}Ge_{0.25})B₂ as a new permanent magnet material. Samples were made by arc-melting/annealing as well as by melt-spinning/annealing and were evaluated by probing the structure, composition, and magnetic response. Results indicate that the tetragonal Cr₅B₃ crystal structure, large saturation magnetization ($M_s = 153.8$ emu/g) and Curie temperature ($T_c = 784$ K) of the parent Fe₅SiB₂ phase may be preserved by substituting up to 25 at % of Si in the lattice with Ge. The room-temperature magnetocrystalline anisotropy constant of a Ge-substituted alloy of nominal composition Fe₅(Si_{0.75}Ge_{0.25})B₂ was evaluated as $K_1 = 5 \times 10^6$ ergs/cc using the law of approach to saturation and is the largest reported to date within the 5-1-2 materials system. As a result of compositional modification, the spin reorientation observed in Fe₅SiB₂ is greatly suppressed from 172 K to 60 K. A comparison of the 5-1-2 phase evolution when synthesized by standard casting and by rapid solidification indicates that melt spinning is a simpler and more expeditious synthesis method relative to previously reported solid-state reaction methods.

© 2017 Elsevier B.V. All rights reserved.

1. Introduction

Motivation persists to diversify the supply and increase the availability of high-performance magnets in response to ever-growing demand in the energy, defense, transportation and consumer product sectors [1,2]. To this end, it is desired to develop novel Fe-based intermetallic compounds with a large magnetization, high Curie temperature, and appreciable uniaxial magnetocrystalline anisotropy that can donate high coercivity. While the Fe₅SiB₂ (5-1-2) compound has been reported to exhibit a high saturation magnetization ($M_s = 153.8$ emu/g) and a Curie temperature in excess of 750 K, it possesses a technologically low anisotropy energy at room temperature ($K_1 = 2.5\text{--}3.0 \times 10^6$ ergs/cc), as determined by the law of approach to saturation [3–7].

These features motivate research towards controlling the anisotropy of this compound using intrinsic (compositional) and extrinsic (microstructural control) means. The Fe₅SiB₂ compound has the tetragonal Cr₅B₃ prototypical layered structure (space group *I4/mcm*; $a = 5.5507$ (1) Å and $c = 10.3359$ (2) Å) with bi-capped tetragonal antiprisms comprised of a cage of ten Fe atoms enclosing a Si atom, Fig. 1 [3]. A uniaxial magnetization along the *c*-axis exists for $T > 172$ K which marks the spin reorientation temperature T_{sp} ; for $T < T_{sp}$ the compound adopts an easy-plane anisotropy [3,4].

Chemical substitution has been confirmed to enhance the magnetocrystalline anisotropy in many intermetallic ferromagnetic systems [2,8–13]. Efforts to compositionally engineer the magnetocrystalline anisotropy in the 5-1-2 system indicate that substitution of Mn for Fe has no apparent effect, while computational results conclude that the substitution of Co for Fe, as well as P and S for Si in the Fe₅SiB₂ structure increases the anisotropy energy [3,5]. Preservation of the Cr₅B₃ structure type is reported in all these studies. For substitutions of Co for Fe and P for Si, this increased

* Corresponding author. Department of Chemical Engineering, Northeastern University, Boston, MA 02115, USA.

E-mail address: lejeune.b@husky.neu.edu (B.T. Lejeune).

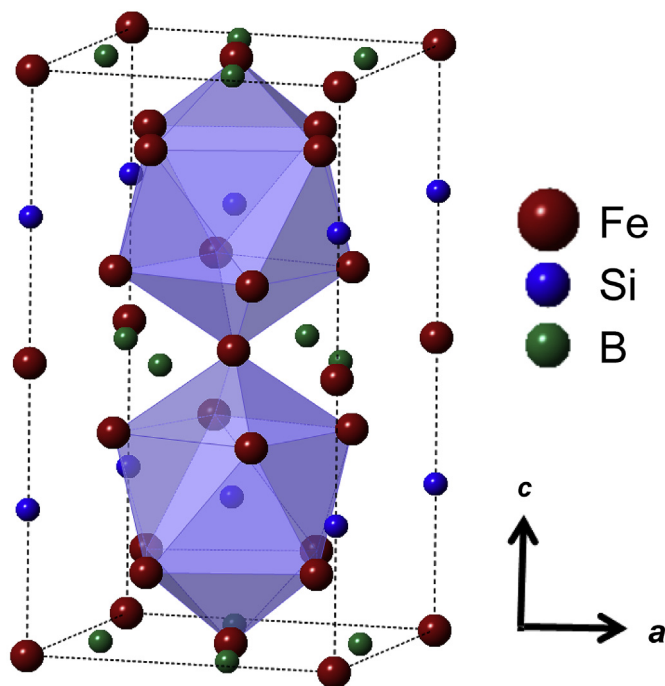


Fig. 1. Fe_5SiB_2 (Cr_5B_3 type) unit cell depicting bi-capped tetragonal antiprisms shown in blue which are formed from a 10 Fe atom cage enclosing a Si atom. (For interpretation of the references to colour in this figure legend, the reader is referred to the web version of this article.)

anisotropy energy is accompanied by a decrease in the Curie temperature (to 675 K and to 640 K, respectively) and a decreased saturation magnetization (to 112.2 emu/g and to 124.8 emu/g, respectively) [3,5]. The effects of sulfur substitution for silicon in the lattice on the Curie temperature and saturation magnetization were not reported [5]. In all cases it is reported that elemental substitution from the parent Fe_5SiB_2 structure suppresses the spin reorientation temperature.

In this current work, changes in the magnetic properties of Fe_5SiB_2 due to the incorporation of small amounts of Ge are reported. Additionally, the impact of solidification rate during synthesis from the melt on the 5-1-2 magnetic and structural properties are also documented. It is determined that the room-temperature anisotropy energy of $\text{Fe}_5(\text{Si}_{0.75}\text{Ge}_{0.25})\text{B}_2$ is the largest of any 5-1-2 compound reported to date. Moreover, it is shown that rapid solidification of the compound by melt-spinning and subsequent annealing requires far less time and effort for synthesis of this phase compared to previously reported solid state reaction techniques [3]. These results are assessed in the context of the potential of the Fe_5SiB_2 family of compounds for advanced permanent magnet applications.

2. Methods

Chemically-modified Fe_5SiB_2 samples of composition $\text{Fe}_5(\text{Si}_{0.75}\text{Ge}_{0.25})\text{B}_2$, were synthesized by standard arc-melting to produce cast ingots as well as by rapid solidification via melt-spinning to produce thin ribbons. The $\text{Fe}_5(\text{Si}_{0.75}\text{Ge}_{0.25})\text{B}_2$ ingots were prepared by arc-melting the constituent elements (99.9% purity) in an inert Ar atmosphere. A portion of the $\text{Fe}_5(\text{Si}_{0.75}\text{Ge}_{0.25})\text{B}_2$ arc-melted charge was subsequently melt-spun on a water-cooled copper wheel in Ar at a tangential wheel speed of 30 m/s to produce brittle ribbons of approximately 2–3 mm in width and 5–10 cm in length. Both ingots and ribbons were sealed under vacuum (1×10^{-6} Torr)

in vitreous silica tubes and annealed using the following conditions: $T = 1000^\circ\text{C}/10$ days for cast samples and $T = 600^\circ\text{C}/1$ h for melt-spun samples; the tubes were quenched in ice water after the annealing treatments. The annealing temperatures were chosen on the basis of calorimetric data, described below, that provides information regarding stability of the 5-1-2 phase in these two forms of materials.

The chemical composition and homogeneity of both types of sample were confirmed before annealing using energy-dispersive x-ray spectrometry in a scanning electron microscope (SEM-EDS, Hitachi S4800). Samples were ground to a powder ($<45\ \mu\text{m}$) in air for structural characterization using standard laboratory x-ray powder diffractometry ($\text{Cu-K}\alpha$ radiation, $\lambda = 1.54184\ \text{\AA}$; PAN-analytical X'Pert PRO and Rigaku Ultima III). Bragg reflections obtained from the x-ray diffraction patterns were fit with a pseudo-Voigt function and indexed to a simulated tetragonal unit cell of the Cr_5B_3 ($I4/mcm$) structure type. This simulated Fe_5SiB_2 pattern was generated with VESTA using known lattice parameters and atomic positions from the literature [3,14]. Lattice parameters of the $\text{Fe}_5(\text{Si}_{0.75}\text{Ge}_{0.25})\text{B}_2$ samples were determined using a least-squares fit [15]. The approximate crystallite size (τ) of phase was assessed using the Scherrer formula

$$\tau = \frac{0.9 \cdot \lambda}{\beta \cos \theta} \quad [1]$$

where $\lambda = 1.54184\ \text{\AA}$ is the wavelength of $\text{Cu-K}\alpha$ radiation, β is the full width at half maximum of the main (213) diffraction peak, and θ is the Bragg peak position [16].

Magnetic characterization of isotropic powdered samples was carried out using Vibrating Sample Magnetometry (VSM, Quantum Design model VersaLab) in magnetic fields up to $\mu_0 H_{\text{app}} = 3\ \text{T}$ and temperatures in the range $50\ \text{K} \leq T \leq 1000\ \text{K}$ as well as using a Superconducting Quantum Interference Device or SQUID magnetometer (Quantum Design model MPMS) in magnetic fields up to $\mu_0 H_{\text{app}} = 0.01\ \text{T}$ and temperatures in the range $10\ \text{K} \leq T \leq 300\ \text{K}$. Data were corrected for demagnetization effects attributed to the cylindrical sample geometries [7,17]. The Curie temperature (T_c) of the samples was determined as the inflection point of magnetothermal data collected upon heating (i.e., as the minimum in the dM/dT vs. T data). The spin reorientation temperature (T_{sp}) was determined as the peak of low-temperature magnetothermal data collected upon heating ($10\ \text{K} < T < 300\ \text{K}$) in an applied magnetic field of 100 Oe after zero-field-cooling (ZFC) and after field-cooling (FC) in an applied magnetic field of 100 Oe to $T = 10\ \text{K}$.

The law of approach to saturation was employed to calculate the anisotropy constant (K_1) based on the slope of H_{app}^2 versus magnetization (M) at high field and 300 K with the following equations:

$$\frac{M(H)}{M_S} = \left(1 - \frac{b}{H_{\text{app}}^2} \right) \quad [2]$$

where

$$b = \frac{4}{15} \frac{K_1^2}{J_S^2} \quad [3]$$

where J_S is the magnetization in emu/cc calculated from M_S using the density of the sample, taken as $6.864\ \text{g/cm}^3$ [3,4,7]. As introduced by Coey, a metric to assess the performance of potential permanent magnet materials termed the hardness parameter κ was calculated from the determined anisotropy constant as follows:

$$\kappa = \sqrt{K_1 / 4\pi J_s^2} \quad [4]$$

where K_1 is the anisotropy constant in ergs/cc, J_s is the volume magnetization in emu/cc, and κ the hardness parameter is dimensionless [18]. The maximum coercivity attainable has been calculated from the K_1 value using the formula:

$$H_C \cong \frac{2K_1}{J_s} \quad [5]$$

where H_C is the coercive field in Oe, K_1 is the anisotropy constant in erg/cc, and J_s is the saturation magnetization in emu/cc [18].

Information concerning the phase transformation character of the as-cast ingots and as-spun ribbons was obtained by calorimetry ((NETSCH STA 449 F3 *Jupiter*) performed upon both heating and cooling in the temperature range $300 \text{ K} \leq T \leq 1000 \text{ K}$ at a temperature sweep rate of 15 K/min with Ar as the carrier gas. The onset temperatures of detected phase transitions were determined using the equipment software as the intersection of tangents extended from the baseline and from the leading edge of the exothermic or endothermic peaks in the calorimetric data.

3. Results

Results pertaining to the structural and magnetic properties of $\text{Fe}_5(\text{Si}_{0.75}\text{Ge}_{0.25})\text{B}_2$ are presented for both cast/annealed and melt-spun/annealed samples and are compared with properties of the parent Fe_5SiB_2 phase as provided in the literature [3–5]. Additionally, the calorimetric data of rapidly-solidified $\text{Fe}_5(\text{Si}_{0.75}\text{Ge}_{0.25})\text{B}_2$ samples are presented that provide evidence that melt-spinning is a more streamlined and faster method of 5-1-2 synthesis than standard solid-state synthesis.

3.1. Structure and phase transformation behavior of $\text{Fe}_5\text{Si}_{0.75}\text{Ge}_{0.25}\text{B}_2$

XRD data of cast/annealed $\text{Fe}_5(\text{Si}_{0.75}\text{Ge}_{0.25})\text{B}_2$ (Fig. 2(a)) confirm attainment of the Cr_5B_3 structure with no minor phases detected ($a = 5.551(1) \text{ \AA}$, $c = 10.347(1) \text{ \AA}$) [3–5]. The sample appears to be highly crystalline with a grain size of approximately 80 nm. Compositional analysis carried out on the cast/annealed form of $\text{Fe}_5(\text{Si}_{0.75}\text{Ge}_{0.25})\text{B}_2$ confirms that the phase contains 3 at% Ge and

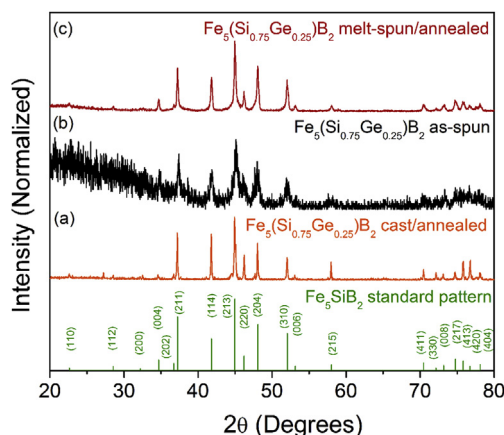


Fig. 2. (a) XRD data of cast/annealed Ge-substituted $\text{Fe}_5(\text{Si}_{0.75}\text{Ge}_{0.25})\text{B}_2$ with Cr_5B_3 structure type. (b) XRD data of as-spun Ge-substituted $\text{Fe}_5(\text{Si}_{0.75}\text{Ge}_{0.25})\text{B}_2$ ribbons that indicates poor crystallinity, while (c) melt-spun/annealed ribbons showed good crystallinity.

9.5 at% Si which is within experimental error of the nominal composition. XRD data obtained from the as-spun samples (Fig. 2(b)) indicate attainment of the Cr_5B_3 -type structure ($a = 5.559(4) \text{ \AA}$, $c = 10.325(5) \text{ \AA}$), but with poor crystallinity, possessing a grain size on the order of 15 nm. Annealing of as-spun samples preserves the 5-1-2 crystal structure ($a = 5.549(1) \text{ \AA}$, $c = 10.337(5) \text{ \AA}$), Fig. 2(c), and improves the crystallinity of the melt-spun ribbons (grain size ~40 nm). Overall, the crystallographic properties (lattice parameters, tetragonality as quantified by the calculated c/a ratio, and grain size) of the cast/annealed and melt-spun/annealed $\text{Fe}_5(\text{Si}_{0.75}\text{Ge}_{0.25})\text{B}_2$ samples, summarized in Table 1, were found to be comparable with those of the parent unmodified Fe_5SiB_2 compound [3–5].

Calorimetry data shown in Fig. 3 documents the thermal response of as-spun $\text{Fe}_5(\text{Si}_{0.75}\text{Ge}_{0.25})\text{B}_2$ upon heating and cooling. A large irreversible exothermic peak is observed at $T_{\text{onset}} = 800 \text{ K}$ upon heating the as-spun ribbon; this feature is not observed in the cast form of $\text{Fe}_5(\text{Si}_{0.75}\text{Ge}_{0.25})\text{B}_2$ either in the pre- or the post-anneal states.

3.2. Magnetic character of $\text{Fe}_5\text{Si}_{0.75}\text{Ge}_{0.25}\text{B}_2$

The temperature-dependent magnetization of cast/annealed $\text{Fe}_5(\text{Si}_{0.75}\text{Ge}_{0.25})\text{B}_2$ drops continuously from a high-magnetization (ferromagnetic) state to a low-magnetization (paramagnetic) state, Fig. 4. The Curie temperature of the cast/annealed sample ($T_C = 791 \pm 1 \text{ K}$) is higher than that of the unmodified parent phase ($T_C = 784 \text{ K}$) [3,4,6]. The Ge-substituted cast/annealed sample has a room-temperature saturation magnetization value ($M_S = 134.4 \text{ emu/g}$) that is smaller than that of the parent unmodified Fe_5SiB_2 compound ($M_S = 153.8 \text{ emu/g}$), shown in Table 2 [3]. A small coercive field of ~20 Oe is observed in this sample at room temperature. The Curie temperature ($T_C = 793 \text{ K}$) and room temperature saturation magnetization ($M_S = 158.3 \text{ emu/g}$) values of melt-spun/annealed Ge-containing ribbons, Fig. 4, correspond well with those measured from the cast/annealed $\text{Fe}_5(\text{Si}_{0.75}\text{Ge}_{0.25})\text{B}_2$ specimen as well as the reference values of Fe_5SiB_2 parent compound. The room-temperature coercive field in the melt-spun/annealed sample is on the order of ~150 Oe.

Fig. 5 shows the ZFC/FC thermomagnetization curve of the cast/annealed $\text{Fe}_5(\text{Si}_{0.75}\text{Ge}_{0.25})\text{B}_2$ sample, indicating a spin reorientation temperature of 60 K. This transition temperature is suppressed from 172 K in the unmodified sample [4]. The difference between the ZFC and FC curves for $T > T_{sp}$ is attributed to the difference in magnetization at the applied field as a result of the coercivity of the compound. The melt-spun/annealed sample did not show evidence of a spin reorientation for $T > 10 \text{ K}$.

The determined room-temperature anisotropy constants (K_1) of both cast/annealed and melt spun/annealed $\text{Fe}_5(\text{Si}_{0.75}\text{Ge}_{0.25})\text{B}_2$ are included in Table 2, with values $3.5 \times 10^6 \text{ ergs/cc}$ and $5 \times 10^6 \text{ ergs/cc}$, respectively. It is noted that these values are significantly larger than that of the parent phase ($K_1 = 2.5\text{--}3 \times 10^6 \text{ ergs/cc}$) [5]. Fig. 6(a) and (b) show the room temperature $1/H_{app}^2$ vs M plot at high field of the cast/annealed and melt-spun/annealed samples used for determining the anisotropy constants. The hardness parameter has been calculated for the parent phase ($\kappa \sim 0.4$) and $\text{Fe}_5\text{Si}_{0.75}\text{Ge}_{0.25}\text{B}_2$ samples ($\kappa \sim 0.6$), shown in Table 2.

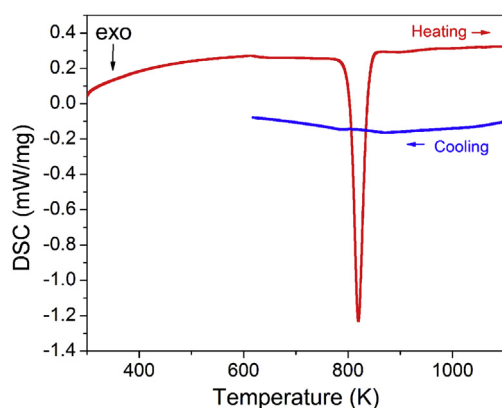
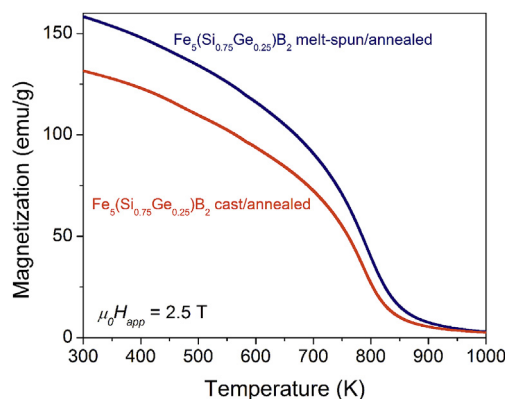
4. Discussion

Effects of the substitution of 25 at% Ge for Si in the 5-1-2 compound on the structural and magnetic behavior of Fe_5SiB_2 are discussed, and comparisons of phase synthesis by conventional and rapid solidification techniques are presented.

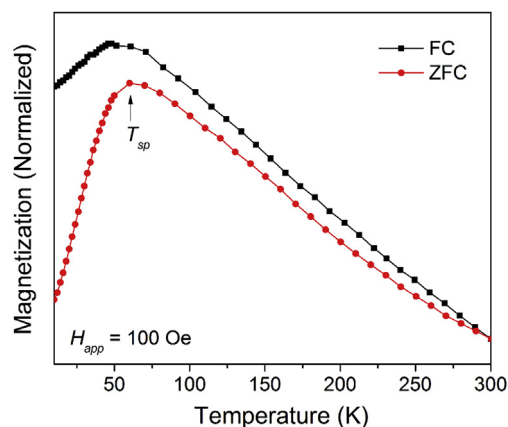
While Ge is confirmed by EDS to substitute into the 5-1-2 lattice,

Table 1Lattice parameters and grain sizes determined for $\text{Fe}_5(\text{Si}_{0.75}\text{Ge}_{0.25})\text{B}_2$ samples. The reported values for the parent phase Fe_5SiB_2 are included for reference.

Sample Name	Form	a (Å)	c (Å)	c/a	V (Å ³) \pm 1% error	Approx. grain size (nm)
Fe_5SiB_2 [4]	Cast/annealed	5.561 (1)	10.348 (1)	1.86	319	—
Fe_5SiB_2 [5]	Cast/annealed	5.546	10.341	1.86	318	—
Fe_5SiB_2 [3]	Cast/annealed	5.551 (1)	10.336 (2)	1.86 (1)	319	—
$\text{Fe}_5(\text{Si}_{0.75}\text{Ge}_{0.25})\text{B}_2$	Cast/annealed	5.551 (1)	10.347 (1)	1.86 (1)	319	80
$\text{Fe}_5(\text{Si}_{0.75}\text{Ge}_{0.25})\text{B}_2$	As melt-spun	5.559 (4)	10.325 (5)	1.86 (1)	319	15
$\text{Fe}_5(\text{Si}_{0.75}\text{Ge}_{0.25})\text{B}_2$	Melt-spun/ annealed	5.549 (1)	10.337 (1)	1.86 (1)	318	40

**Fig. 3.** Calorimetric response for melt-spun $\text{Fe}_5\text{Si}_{0.75}\text{Ge}_{0.25}\text{B}_2$ exhibits an irreversible exothermic peak with $T_{\text{onset}} \sim 800$ K.**Fig. 4.** Magnetization versus temperature $M(T)$ above room-temperature for Ge substituted samples. Annealed melt-spun/annealed ribbons $M(T)$ behavior is similar to that of cast/annealed Ge samples with a Curie temperature of 793 K.

it does not greatly impact the lattice parameters, the Curie temperature nor the saturation magnetization relative to the parent compound. However, this Ge addition does suppress the spin reorientation temperature T_{sp} to 60 K, greatly reduced from the value of $T_{\text{sp}} = 172$ K reported for the parent compound [11,13]. It is proposed that Ge substitutes in the lattice position that separates

**Fig. 5.** Magnetization versus temperature $M(T)$ below room temperature for cast/annealed $\text{Fe}_5(\text{Si}_{0.75}\text{Ge}_{0.25})\text{B}_2$. Zero-field-cooled (ZFC) and field-cooled (FC) measurements show a spin reorientation in $\text{Fe}_5(\text{Si}_{0.75}\text{Ge}_{0.25})\text{B}_2$ which is suppressed from $T = 172$ K–60 K.

the Fe-B tetragonal antiprisms but participates only minimally in the Fe-Fe and Fe-B magnetic exchange within the unit cell [3,5]. These observations, along with the measured 3:1 Si to Ge atomic ratio in the phase pure $\text{Fe}_5\text{Si}_{0.75}\text{Ge}_{0.25}\text{B}_2$ samples, support the hypothesis that the introduced Ge substitutes for Si within the 5-1-2 structure.

The determined magnetocrystalline anisotropy energy value of 5.0×10^6 ergs/cc for the $\text{Fe}_5(\text{Si}_{0.75}\text{Ge}_{0.25})\text{B}_2$ compound is the largest experimental value reported to date for any member of the 5-1-2 iron silicides. The 25 at% Ge modification donates a two-fold increase in the magnetocrystalline anisotropy energy, to 5.0×10^6 ergs/cc from that of the unmodified compound value of $2.5\text{--}3.0 \times 10^6$ ergs/cc. At this time, the observed larger anisotropy constant and suppression of the spin reorientation temperature in the melt-spun/annealed sample relative to the cast/annealed sample, Table 2, is attributed to microstructural effects, such as the smaller grain size obtained in the melt-spun/annealed sample (40 nm vs. 80 nm) [19]. The reduction in T_{sp} is attributed to bonding alterations due to Ge substitutions that change the magnitude and thermal dependence of the magnetocrystalline anisotropy constants, thus modifying the temperature at which the sign of K_1 inverts in $\text{Fe}_5(\text{Si}_{0.75}\text{Ge}_{0.25})\text{B}_2$, relative to Fe_5SiB_2 .

Results indicate that high-quality Ge-containing iron-silicide 5-

Table 2Magnetic properties of Ge-substituted samples categorized according to synthesis method and compared to the parent phase Fe_5SiB_2 .

Sample Name	Synthesis Method	M_s (emu/g) \pm 1% error	T_C (K) \pm 0.5% error	T_{SP} (K)	K_1 approach to saturation (ergs/cc) \pm 10% error	κ hardness parameter
Fe_5SiB_2	Solid state reaction	153.8 [3]	784 [3,6]	172 [3,4]	2.5×10^6 [5]	0.42
$\text{Fe}_5(\text{Si}_{0.75}\text{Ge}_{0.25})\text{B}_2$	As-spun	116	794	—	2.9×10^6	0.60
$\text{Fe}_5(\text{Si}_{0.75}\text{Ge}_{0.25})\text{B}_2$	Melt-spun/annealed	158.3	793	—	5.0×10^6	0.58
$\text{Fe}_5(\text{Si}_{0.75}\text{Ge}_{0.25})\text{B}_2$	Cast/annealed	134.4	791	60	3.5×10^6	0.57

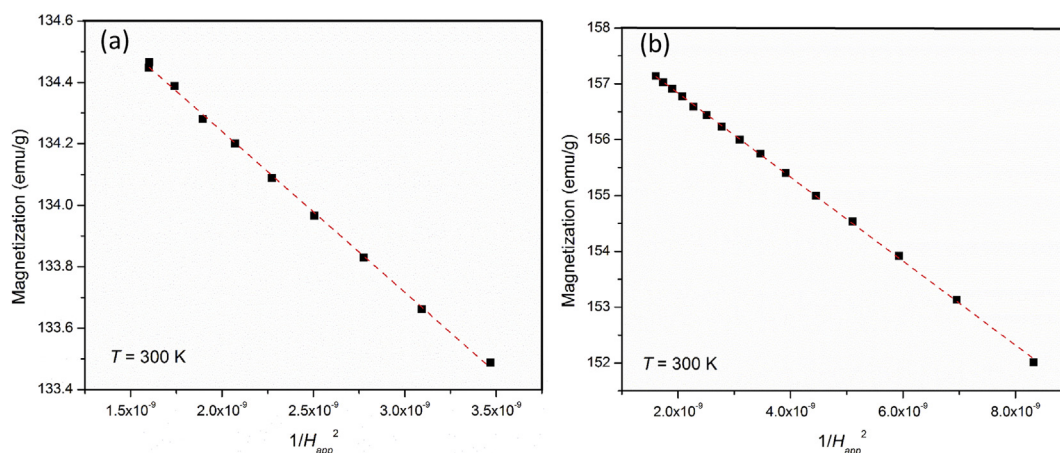


Fig. 6. Magnetization versus $1/H_{app}^2$ at 300 K in the high magnetic field region used to calculate the anisotropy constant K_1 using the law of approach to saturation for $\text{Fe}_5(\text{Si}_{0.75}\text{Ge}_{0.25})\text{B}_2$ (a) cast/annealed and (b) melt-spun/annealed samples.

1-2 compounds may be easily and rapidly obtained, an advantage over those made by solid-state reaction methods, as reported by McGuire and Parker [3]. As shown in Table 2, the lattice parameters and the measured magnetic transition temperature of Ge-containing melt-spun/annealed ribbons coincide with those of the cast/annealed samples. It is ascertained that melt-spun samples formed by rapid solidification of the 5-1-2 iron silicide phase produce a nanocrystalline structure with a substantial amorphous component that crystallizes at $T = 800$ K upon heating, Fig. 3. The rapid crystallization observed facilitates the short annealing times of melt-spun ribbons, on the order of 1 h.

With relevance to permanent magnet applications, it must be noted that the Ge-substituted 5-1-2 samples possess a hardness factor 50% larger than that of the parent compound ($\kappa \sim 0.6$ and $\kappa \sim 0.4$, respectively). Utilizing Eq. (5), a calculated ideal coercivity value in excess of 9 kOe at $T = 300$ K suggests that the measured coercivity may be increased in the samples via microstructural tailoring. At this time the Fe_5SiB_2 system is not optimized for permanent magnet applications where hardness parameter $\kappa > 1$ is desired [18]. Nonetheless, this study provides insight of both fundamental and applied relevance concerning pathways for maximizing the permanent magnet potential of Fe_5SiB_2 for applications in the power and energy sector.

5. Conclusions

This study confirms the substitution of Ge for Si in the Fe_5SiB_2 compound, leading to an increase in the magnetocrystalline anisotropy from $2.5\text{--}3.0 \times 10^6$ ergs/cc to 5.0×10^6 ergs/cc. Additionally, Ge substitution allows the Fe_5SiB_2 system to maintain a high Curie temperature and large saturation magnetization, unlike many elemental substitutions reported in the literature. By developing novel synthesis pathways for this material system through melt-spinning, the complexity of solid-state reaction synthesis and processing protocols traditionally used to produce phase pure 5-1-2 samples can be avoided, and the time required for high-quality phase attainment may be greatly reduced. The results of this work suggest that additional compositional adjustments (intrinsic modification) and microstructural refinement (extrinsic modification) may allow tailoring of the magnetization and magnetocrystalline anisotropy within the Fe_5SiB_2 system to enhance its permanent magnet potential.

Acknowledgements

Research was funded by Northeastern University, by the Army Research Office under grant number W911NF-10-2-0098, subaward 15-215456-03-00; and by the US Department of Energy grant number FG02-90ER45413.

References

- [1] L.H. Lewis, F. Jiménez-Villacorta, Perspectives on permanent magnetic materials for energy conversion and power generation, *Metall. Mater. Trans. A* 44 (2012), <https://doi.org/10.1007/s11661-012-1278-2>.
- [2] R.W. McCallum, L.H. Lewis, R. Skomski, M.J. Kramer, I.E. Anderson, *Practical Aspects of Modern and Future Permanent Magnets*, 2014, <https://doi.org/10.1146/annurev-matsci-070813-113457>.
- [3] M.A. McGuire, D.S. Parker, Magnetic and structural properties of ferromagnetic Fe_5PB_2 and Fe_5SiB_2 and effects of Co and Mn substitutions, *J. Appl. Phys.* 118 (2015), <https://doi.org/10.1063/1.4934496>.
- [4] J. Cedervall, T.C. Hansen, O. Balmes, F.J. Martinez-Casado, Z. Matej, P. Beran, P. Svedlindh, K. Gunnarsson, M. Sahlberg, Magnetostructural transition in Fe_5SiB_2 observed with neutron diffraction, *J. Solid State Chem.* 235 (2016) 113–118, <https://doi.org/10.1016/j.jssc.2015.12.016>.
- [5] M. Werwinski, S. Kontos, K. Gunnarsson, P. Svedlindh, J. Cedervall, V. Hoglin, M. Sahlberg, A. Edstrom, O. Eriksson, J. Ruz, Magnetic properties of Fe_5SiB_2 and its alloys with P, S, and Co, *Phys. Rev. B* 93 (2016) 1–10, <https://doi.org/10.1103/PhysRevB.93.174412>.
- [6] R. Wappling, T. Ericsson, L. Haggstrom, Y. Andersson, Magnetic Properties of Fe_5SiB_2 and related compounds, *J. Phys. Colloq.* 37 (1976) 591–593.
- [7] R.M. Bozorth, *Ferromagnetism*, eighth ed., van Nostrand, Princeton, New Jersey, 1951.
- [8] V. Sharma, P. Manchanda, R. Skomski, D.J. Sellmyer, A. Kashyap, Anisotropy of heavy transition metal dopants in Co, *J. Appl. Phys.* 109 (2011) 1–3, <https://doi.org/10.1063/1.3562256>.
- [9] S.D. Willoughby, J.M. MacLaren, T. Ohkubo, S. Jeong, M. McHenry, D. Laughlin, S. Choi, S. Kwon, Electronic, magnetic, and structural properties of $\text{L}_{10}\text{FePtPd}_{1-x}$ alloys, *J. Appl. Phys.* 91 (2002) 8822–8824, <https://doi.org/10.1063/1.1450850>.
- [10] J.M. MacLaren, S.D. Willoughby, M.E. McHenry, B. Ramalingam, S.G. Sankar, First principles calculations of the electronic structure of $\text{Fe}_{1-x}\text{Co}_x\text{Pt}$ Co Pt Structure of Fe, *IEEE Trans. Magn.* 37 (2001) 1277–1279, <https://doi.org/10.1109/20.950817>.
- [11] S. Kauffmann-Weiss, S. Hamann, M.E. Gruner, L. Schultz, A. Ludwig, S. Fahler, Enhancing magnetocrystalline anisotropy of the $\text{Fe}_{70}\text{Pd}_{30}$ magnetic shape memory alloy by adding Cu, *Acta Mater.* 60 (2012) 6920–6930, <https://doi.org/10.1016/j.actamat.2012.08.001>.
- [12] R. Skomski, A. Kashyap, A. Solanki, A. Enders, D.J. Sellmyer, Magnetic anisotropy in itinerant magnets, *J. Appl. Phys.* 107 (2010) 1–4, <https://doi.org/10.1063/1.3339780>.
- [13] J. Cui, T.W. Shield, R.D. James, Phase transformation and magnetic anisotropy of an iron – palladium ferromagnetic shape-memory alloy, *Acta Mater.* 52 (2004) 35–47, <https://doi.org/10.1016/j.actamat.2003.08.024>.
- [14] K. Momma, F. Izumi, VESTA 3 for three-dimensional visualization of crystal, volumetric and morphology data, *J. Appl. Crystallogr.* 44 (2011) 1272–1276.
- [15] G.A. Novak, A.A. Colville, A practical interactive least-squares cell-parameter

- program using an electronic spreadsheet and a personal computer, *Am. Mineral.* 74 (1989) 488–490.
- [16] B.D. Cullity, *Elements of X-ray Diffraction*, second ed., Addison Welsley publishing company, 1978.
- [17] D. Chen, J.A. Brug, R.B. Goldfarb, Demagnetizing factors for cylinders, *IEEE Trans. Magn.* 27 (1991) 3601–3619.
- [18] J.M.D. Coey, Permanent magnets: plugging the gap, *Scr. Mater.* 67 (2012) 524–529, <https://doi.org/10.1016/j.scriptamat.2012.04.036>.
- [19] L.H. Lewis, C.L. Harland, *Field Dependence of the Spin Reorientation Temperature in Micro- and Nanocrystalline Forms of Nd₂Fe₁₄B*, 2003.